IJR International Journal of Railway
Vol. 8, No. 2 / June 2015, pp. 35-41

The Korean Society for Railway

Settlement and Bearing Capacity of Roadbed Subjected to Tilting-train Loading in Various Ground Conditions

Sang-Soo Jeon†

Abstract

Tilting-train is very attractive to the railroad users in the world due to the advantage of high speed in curved track using pre-existing infrastructure of railway. Tilting-train has a unique allowable speed and mechanism especially in curved track. In this work, when tilting-train is operated with the allowable speed, the behavior of roadbed is evaluated by examining its settlement and bearing capacity. Additionally, the stability of roadbed is estimated as the roadbed is in the condition of soft soil influenced by the weather effects and cyclic train loading. Numerical results show that the roadbed settlement satisfies the allowable settlement when the elastic modulus of upper roadbed should be greater than 5000 t/m^2.

Keywords: *Numerical analysis, Railway, Tilting-train, Bearing capacity, Settlement*

1. Introduction

Railway has an important role on transportation systems but the development of automobile and airplane industries has been developed with large amount of budgets with the railway industry retarded. However, in recent years, the important role of railways such as large amount of transportation, stability, energy efficiency, and prevention of environmental problems has been raised [1]. Railway among high competitive transportation systems has been developed with high speed and stability.

Tilting-train, which is operated in tilted towards inside in curved track with high speed, has been developed to provide the express service system by using the existing railways. A general introduction to the concept of tilt, the limit to tilt application, the curving speed of a tilting train, and performance advantages of tilt were discussed [2]. Since the capacity and operation condition of the tilting-train especially in curved track are unique, the allowable speed has been proposed with regard to the stability including the roadbed and bearing of track during its operation. The roadbed settlements due to the insufficient bearing of track influenced by the repetitive loadings of the train and the reduced ground stiffness by seasonal temperature changes may cause the derailment and track irregularity. Therefore, in this work, the stability of the track and roadbed during tilting-train operation is examined with respect to various ground conditions.

Numerical modeling has been carried out to simulate the propagation of the vibration waves induced by railway vehicle using finite element analyses and field experiments have been performed to examine the behavior of ground vibrations and also to validate the numerical results [3-8]. In this work, A 2-D finite difference model using the commercial program FLAC^{2D} [9] was adopted to examine the roadbed settlement under tilting-train loadings in various stiffness of roadbed and in-situ soil.

2. Characteristics of Railway Roadbed

Roadbed should strongly support the track with an adequate elasticity with stiffness and distribute the train loads to in-situ soil. Self-weight and vibratory loading of tilting-train due to wheel passage over the rail were transferred to roadbed through a sequence of rail, sleeper, and ballasts.

† Corresponding author: Department of Civil & Environmental Engineering Inje University, Korea
E-mail : ssj@inje.ac.kr

http://dx.doi.org/10.7782/IJR.2015.8.2.035

Table 1 Design criteria of physical properties of soils used in roadbed [10]

Property	Criterion
Maximum diameter (m)	≤ 25
Percentage of passing No. 200 (%)	≤ 35
Coefficient of uniformity, C_u	≤ 6
Plasticity index, PI	≤ 10
Liquid limit, LL (%)	≤ 35

Roadbed subjected to dynamic loading should be stable to support the track in secure and should be designed to minimize the experience occurring mud pumping, the failure of roadbed surface, its deformation, and the ballast intrusion. As the train load is transferred to roadbed, roadbed transfers the load to in-situ soil with the distributed pressures and it should not exceed the allowable bearing capacity. Materials used in roadbed are, in general, obtained from the excavation areas and rivers with good grade soils and should be compacted in uniform single layer with sufficient bearing capacity and low compressibility satisfying the criteria as listed in Table 1. However, if it is not attainable in the construction sites, the crushed stones have been substituted as roadbed materials. Mud pumping in its layer is to be avoided.

The drain layer of sands and gravels less containing fine soils which is less than 10% of soils, in flat and excavated areas should be constructed underneath roadbed. The thickness of drain layer should be 150 mm and well-graded. The river sand has been used with economic benefit and filtering effect. If the geotextile is used for roadbed material, its internal stability should be carefully examined.

3. Allowable Settlement and Bearing Capacity of Roadbed

Train loading acting on railway mostly induces ground settlement. The loading includes the impact and vibration loading transferred from axle of the train. The vibration loading is induced by bump of the contacted area between rail and wheel. Settlements induced by the fluctuation of ballast and gravel infiltration into roadbed depend on the characteristics of railway and trains. Research results from Railway Technical Research Institute (RTRI) in Japan show that the settlement was mainly affected by roadbeds. Settlement ratio of roadbed to ballast is 0.13 to 0.19 for good condition of roadbed consisted of no unique diameter of sandy soil and is 1.3 to 3.1 for bad condition of roadbed consisted of mudstone, weathered soils, and clay. Settlement of roadbed in bad condition is four times greater than that in good condition and is strongly influenced by train speed in bad condition of roadbed. Allowable settlement was determined by roadbed stability, derailment limit, and ride quality.

Table 2 Allowable bearing capacity under roadbed conditions

Roadbed condition	Allowable bearing capacity (t/m^2)	Soil
Good	30	Well compacted sandy soil
Normal	24	Well compacted clay soil
Bad	15	Soft soil

In general, the allowable settlement of 10 mm has been recommended. The vibratory displacement induces gravels to be loose state and frequent repairs of ballasts and it depends on the railway condition. Therefore, the allowable settlement of 2.5 mm is used to procure additional marginal safety in consideration of compressive displacement of both rail pad and ballasts, settlement of rail, low ride quality, both water inflow and cracks in pavement surface of roadbed.

The allowable bearing capacities proposed by several institutions are categorized and listed in Table 2. As listed in the table, the allowable bearing capacities are 30, 24, and 15 t/m^2 for good, normal, and bad conditions of roadbed, respectively. In this work, roadbed is assumed to be in normal condition with the allowable bearing capacity of 24 t/m^2.

4. Continuous Welded Rail (CWR)

Dynamic behavior of roadbed for continuous welded rail (CWR) was examined using the representative values of cant corresponding to the radius of curved tracks.

A CWR, which has a uniform stiffness by welding rail

Fig. 1 Photo of continuous welded rail (CWR)

Table 3 Specification of tilting train

Tilting train	Value
Axle load (t)	15
Speed (km/h)	200 (Design criteria), 180 (Maximum operating speed)
Effective CG height (m)	1.686
Impact coefficient	0.3 (CWR)

Table 4 Specification of prestressed concrete (PC) sleeper 7 associated with 0.3 m depth of ballast

Dimension	Value
Length (m)	2.45
Width (m)	0.28
Height (m)	0.20
Interval between sleepers (m)	0.58

Table 5 Sector conditions

Parameter	Value
Rail gauge (m)	1.435
Cant (mm)	120
Radius of curve (m)	800

Table 6 Spring coefficients of both rail pad and ballast and coefficient of subgrade reaction of roadbed

Name of coefficient	Value
Vertical spring coefficient of rail pad (t/m)	4750
Vertical spring coefficient of ballast (t/m)	20000
Coefficient of subgrade reaction of roadbed (t/m^3)	7200

joint, has been widely used. As shown in Fig. 1, as rail joint is replaced by CWR, there are so many advantages such as, extension of repair periods, reduction of noise and vibration, increased durability of the parts of rail and train, and good ride quality for high-speed train. However, there are disadvantages such as rail joint expansion induced by the temperature increase and buckling induced by high compressive strength at cross-section in lateral direction.

In this work, numerical analyses were carried out to examine the difference of roadbed effects induced by the impact loadings at railways consisted of CWR. As listed in Tables 3 and 4, the axle load of 15 ton for the tilting-train, the design and maximum speeds of 180 and 200 km/h, respectively, were used for the analyses. As listed in Tables 5 and 6, sector conditions, spring coefficients of both rail pad and ballast, and the coefficient of subgrade reaction of roadbed were selected for this work.

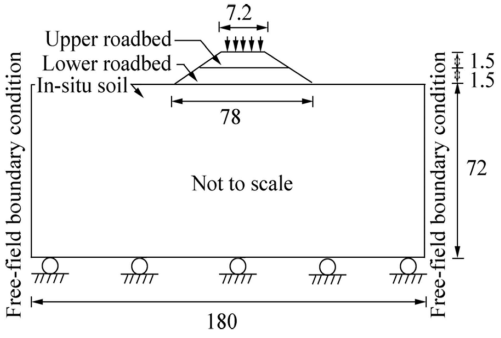

Fig. 2 Configuration of numerical model (unit: m)

5. Numerical Analysis

Dynamic behaviors of roadbed were examined with elasto-plastic Mohr-Coulomb failure model using FLAC^{2D} software as tilting-train was running in curved track. Fig. 2 shows the configurations of numerical model. The embankment height of of upper or lower roadbed, the width of upper roadbed surface, and the slope of the roadbed are 1.5 m, 7.2 m, and 1:1.8, respectively.

It is important to use far-field boundaries at sufficient distance so as not to be influenced by reflective waves of train loading at the boundary. The depth and width of in-situ soil are 72 and 180 m, respectively. The horizontal plane at the bottom of the numerical model was restrained in vertical direction and the boundaries at each lateral side absorb effectively all the incident reflected waves, thereby providing free-field conditions. One of ways not to be influenced by the reflective waves in numerical analysis is to make large size of in-situ soil and lots of meshes but it has a disadvantage of computer inefficiency. Therefore, two boundary conditions to absorb reflective waves which are suggested in FLAC^{2D} model are quiet and free-field conditions. Quiet and free-field boundary conditions were used as the dynamic loading was applied at the location of interior and of boundary, respectively. Since the tilting-train loading was applied at the boundary, the free-field condition was used for this work.

Required time history for the analysis with respect to allowable speed was in the range of 1.413 s associated with the period of 0.059 s for CWR. However, the analysis was performed up to 3 s to examine the characteristics of settlements after the tilting-train passes. The damping ratio of 2 % and the physical properties of soils listed in Table 7 were used for the analysis. Dynamic wheel load and pressures acting on rail and sleeper were calculated and then roadbed pressure was calculated from the pressure distribution in ballasts beneath sleeper.

Table 7 Physical properties of soils

Parameter	Upper roadbed	Lower roadbed	In-situ soil
Unit weight (t/m^3)	1.8	1.8	1.8
Elastic modulus (t/m^2)	5000 8000	4000 6000	6000 10000
Poisson ratio	0.2	0.3	0.3
Cohesion (t/m^2)	0.3	1.0	0.0
Friction angle (°)	32	30	38

5.1 Tilting-train loading

In this work, the pressure at roadbed is transferred from rail and sleeper as tilting-train runs. Dynamic wheel loads and pressures acting on rail and sleeper were calculated from Eqs. (1) to (11) described previously [11] and the pressure acting on roadbed was calculated from the pressure distribution in the areas of ballasts beneath sleeper. Calculation details are explained in the following sections.

5.1.1 Dynamic wheel loads

Dynamic wheel loads in curved track is calculated from the summation of phase-sequence components of both static wheel load and additionally induced wheel load by train speed. The static phase-sequence component of dynamic wheel loads acting on both inside and outside rail associated with the degree of tilt of train is calculated from the summation of bending moment generated at the contact areas between wheel and rail. In this case, the gravity components of arm length of bending moment are changed by the movement of the center of gravity (CG) of tilted train. Degree of tilt proportional to the amount of excess of centrifuge force (cant deficiency, C_d) is equivalent to the increased amount from CG height (H_G) to effective CG height (H_G^*) of the train. Therefore, the static phase-sequence component of wheel loads acting on inside and outside rail in curved track can be explained by Eqs. (1) and (2), respectively.

$$P_{sti} = \frac{w_0}{2}\left[\left(1+\frac{(v/3.6)^2}{gR}\frac{C}{G}\right)-\frac{H_G^*}{G/2}\left[\frac{(v/3.6)^2}{gR}-\frac{C}{G}\right]\right] \quad (1)$$

$$P_{sto} = \frac{w_0}{2}\left[\left(1+\frac{(v/3.6)^2}{gR}\frac{C}{G}\right)+\frac{H_G^*}{G/2}\left[\frac{(v/3.6)^2}{gR}-\frac{C}{G}\right]\right] \quad (2)$$

where P_{sti} is the static phase-sequence component of wheel loads in inside rail (t), P_{sto} is the static phase sequence component of wheel loads in outside rail (t), W_0 is the static axle load (t), G is the distance between inside and outside rails (m), V is the train speed (km/h), C is the cant (m), R is the radius of curved track (m), g is the gravitational acceleration (9.8 m/s^2), and H_G^* is the effective CG height of tilting-train.

$$\Delta P_{sti} = 3[0.5\times P_{sti}\times(i-1)] \quad (3)$$

$$\Delta P_{sto} = 3[0.5\times P_{sto}\times(i-1)] \quad (4)$$

The speed impact (i), 1+α (V/100), is calculated by the speed associated with α=0.3 for CWR. Therefore, the dynamic wheel loads acting on inside and outside rails in curved track is calculated by the summation of static load and additionally induced load by train speed as

$$P_{dyi} = P_{sti} + \Delta P_{sti} \quad (5)$$

$$P_{dyo} = P_{sto} + \Delta P_{sto} \quad (6)$$

5.1.2 Pressure acting on rail

The maximum pressure acting on the rail is estimated when the dynamic wheel loads act on the sleeper and the middle of two sleepers as described in Eqs. (7)-(10).

1) Wheel load acting on the sleeper

$$P_{Ri} = P_{dyi}\left(1-e^{-\beta_i\frac{\alpha}{2}}\cos\beta_i\frac{\alpha}{2}\right) \quad (7)$$

$$P_{Ro} = P_{dyo}\left(1-e^{-\beta_o\frac{\alpha}{2}}\cos\beta_o\frac{\alpha}{2}\right) \quad (8)$$

2) Wheel load acting on the middle of two sleepers

$$P_{Ri} = \frac{P_{dyi}}{2}(1-e^{-\beta_i\alpha}cos\beta_i\alpha) \quad (9)$$

$$P_{Ro} = \frac{P_{dyo}}{2}(1-e^{-\beta_o\alpha}cos\beta_o\alpha) \quad (10)$$

where P_{Ri} is the pressure acting on inside rail (t), P_{Ro} is the pressure acting on outside rail (t), P_{dyi} is the dynamic wheel loads acting on inside rail of curved track (t), P_{dyo} is the dynamic wheel loads acting on outside rail of curved track (t), and is the interval between sleepers (m).

$$\beta_i = \sqrt[4]{\frac{k_i}{4El_x}}, \beta_o = \sqrt[4]{\frac{k_o}{4El_x}}$$

where k_i is the stiffness of inside rail (t/m); k_o is the stiffness of outside rail (t/m); E is the elastic modulus (t/m^2), and I_x is the moment of inertia in x-direction (t·m^2).

5.1.3 Pressure beneath sleeper

As described in Eq. (11), the maximum values of pres-

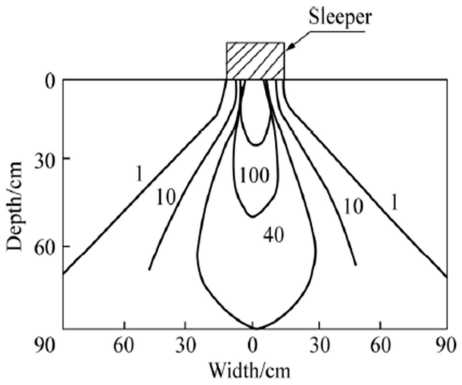

Fig. 3 Pressure distribution in the areas of ballast [11]

sures acting on the rails as the wheel loads act on the sleepers or in the middle of two sleepers were chosen for dynamic analysis.

$$P_t = \frac{P_{Ri_{max}} + P_{Ro_{max}}}{B \times L} \tag{11}$$

where P_t is the pressure beneath sleeper (t/m^2), $P_{Ri_{max}}$ is the maximum pressure in inside rail (t), $P_{Ro_{max}}$ is the maximum pressure in outside rail (t), B is the sleeper width (m), and L is the sleeper length (m).

5.1.4 Roadbed pressure

Roadbed pressure transferred from pressure of underneath sleeper decreases as ballast thickness increases. Roadbed pressure was calculated by using the pressure distribution in the areas of the ballasts [12] as shown in Fig. 3. The maximum pressure in ballasts was found at the center of sleeper and decreases as soil depth and distance from the center of sleeper increase. Numerical analyses were carried out with respect to various radii of curved track and cants associated with allowable speeds determined by both allowable pressure in curved track and running stability of tilting-train. W_o=15 t, H_G^*=1.686 m, G=1.45 m, a=0.58 m, B=0.28 m, and L=2.45 m were used in the analyses.

5.2 Time history of applied tilting-train loading

In this work, cyclic loading of tilting-train was generated by function of regular waves and calculated by amplitude (A), which is the roadbed pressure, associated with frequency of tilting-train loading with respect to time as described in Eq. (12).

$$W(t) = \frac{A}{2} \times (1 - cos 2\pi ft) \tag{12}$$

where A is the amplitude, f is the frequency, 1/T, T is the period, and t is the time.

6. Numerical Results

Seasonal temperature change of roadbed induces repetitive freezing and thawing. It causes its shrinkage and expansion. Since repetitive thermal and train loadings cause soil softening resulting in reduced bearing capacity and stiffness of in-situ soil, the settlements under the reduced elastic modulus of in-situ soil were examined.

Numerical analysis was carried out to examine the roadbed settlement as the tilting-train is operated within the allowable speeds of tilting-train. The allowable settlement was estimated with respect to the cant of 120 mm associated with the radius of curve of 800 m.

The parametric studies were carried out with respect to the elastic moduli of upper roadbed, lower roadbed, and in-situ soil of 5000 and 8000 t/m^2, 4000 and 6000 t/m^2, and 6000 and 10000 t/m^2, respectively. Figs. 4 and 5 show the roadbed settlement with respect to the elasticity of upper and lower roadbed and of in-situ soil. As expected, the settlement exponentially increases as the elasticity of roadbeds and in-situ soil decreases.

As recommended by the design criteria of the railway, the soil reaction modulus, K_{30}, of upper and lower roadbed should be greater than 110 and 70 t/m^2, respectively, where the in-situ soil is stiff enough. However, it was found that the maximum settlement was greater than the allowable settlement of 2.5 mm when the elastic moduli of in-situ soil, upper roadbed, and lower roadbed were 6000, 5000, and 4000 t/m^2, respectively. Fig. 4(a) shows the roadbed settlement. As the load was initially applied to the roadbed surface, the immediate settlement was 1.87 mm and the maximum settlements induced by the continuous repetitive wheel loading was 2.60 mm. The maximum roadbed settlements associated with ground conditions are

Table 8 Roadbed settlement with respect to ground conditions

In-situ soil (t/m^2)	Lower Roadbed (t/m^2)	Upper Roadbed (t/m^2)	Settlement (mm)
6000	4000	5000	2.60
		8000	2.35
	6000	5000	2.51
		8000	2.22
10000	4000	5000	2.19
		8000	1.93
	6000	5000	2.15
		8000	1.81

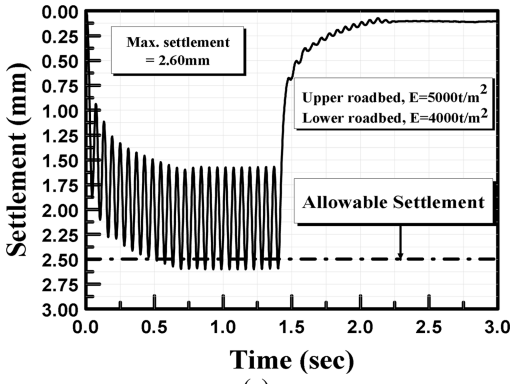

(a)

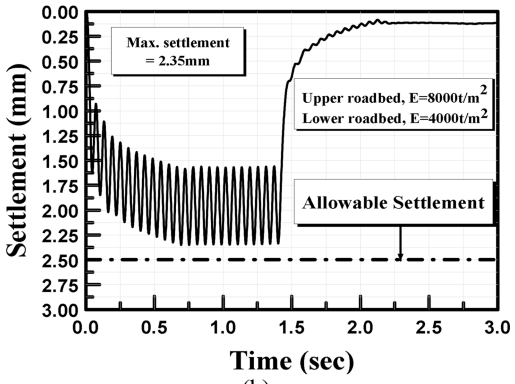

(b)

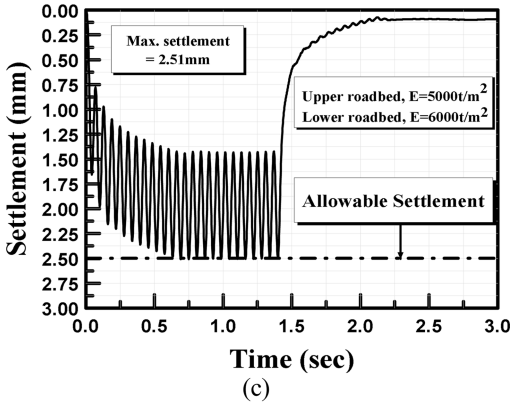

(c)

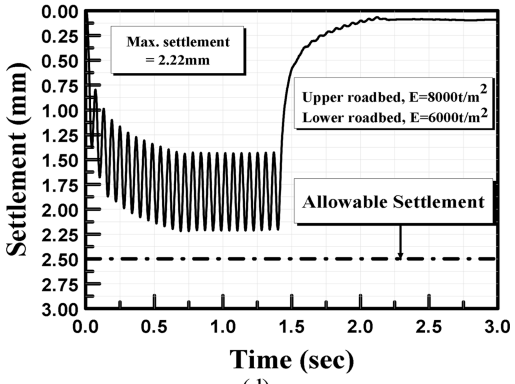

(d)

Fig. 4 Roadbed settlement during tilting-train operation for elastic modulus, E(in-situ soil) = 6000 t/m^2

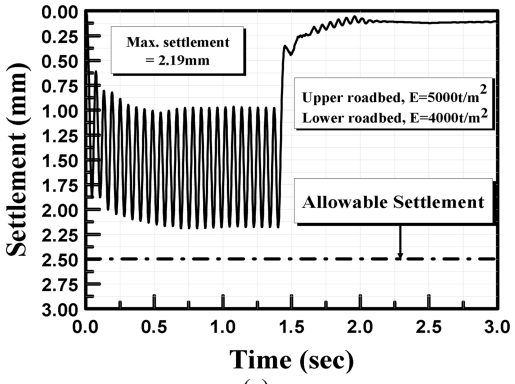

(a)

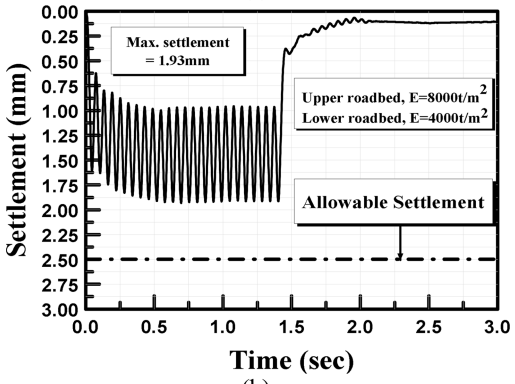

(b)

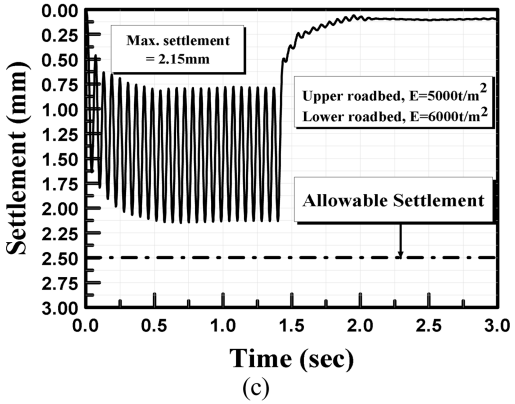

(c)

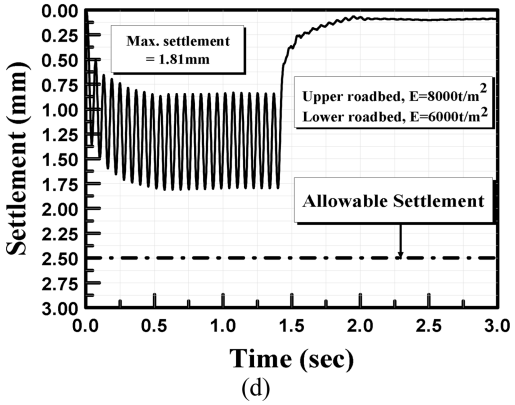

(d)

Fig. 5 Roadbed settlement during tilting-train operation for elastic modulus, E(in-situ soil) = 10000 t/m^2

summarized in Table 8. Therefore, the reinforcement of in-situ soil is recommended to increase its stiffness.

7. Conclusions

Allowable speed was estimated with the typical values of cants associated with the radius of curve, 800 m. The allowable speed was estimated for the radius of curve of 800 m associated with the cant of 120 mm. The maximum settlement was greater than the allowable settlement of 2.5 mm when the elastic moduli of in-situ soil, upper roadbed, and lower roadbed were 6000, 5000, and 4000 t/m^2, respectively. Fig. 4(a) shows the roadbed settlement. As the load was initially applied to the roadbed surface, the immediate settlement was 1.87 mm and the maximum settlements induced by the continuous repetitive wheel loading was 2.60 mm. Since repetitive train and thermal loadings resulting in softening of upper roadbed may cause greater settlement than the allowable settlement, the elastic modulus of upper roadbed greater than 5000 t/m^2 should be maintained not to exceed the allowable settlement.

References

1. Esveld, C. (2001). “Modern railway,” MRT-Productions, pp.1-16.
2. Harris, N. R., Schmid, F., and Smith, R. A. (1998). “Introduction: Theory of tilting train behavior,” Journal of Rail and Rapid Transit, Vol. 212, No. 1, January, pp.1-5.
3. Degrande, G., Clouteau, D., Othman, R., Arnst, M., Chebli, H., Klein, R., Chatterjee, P., and Janssens, B. (2006). “A numerical model for ground-borne vibrations from underground railway traffic based on a periodic finite element-boundary element formulation,” Journal of Sound and Vibration, Vol. 293, No. 3-5, June, pp.645-666.
4. Ju, S. H., Liao, J. R., and Ye, Y. L. (2010). “Behavior of ground vibrations induced by trains moving on embankments with rail roughness,” Soil Dynamics and Earthquake Engineering, Vol. 30, No. 11, November, pp.1237-1249.
5. Kouroussis, G., Verlinden, O., and Conti, C. (2010). “On the interest of integrating vehicle dynamics for the ground propagation of vibrations: The case of urban railway traffic,” Vehicle System Dynamics, Vol. 48, No. 12, January, pp.1553-1571.
6. Paolucci, R., Maffeis, A., Scandella, L., Stupazzini, M., and Vanini, M. (2003). “Numerical prediction of low-frequency ground vibrations induced by high-speed trains at Ledsgaard, Sweden,” Soil Dynamics and Earthquake Engineering, Vol. 23, No. 6, August, pp.425-433.
7. Saussine, G., Cholet, C., Gautier, P. E., Dubois, F., Bohatier, C., and Moreau, J. J., (2006). “Modelling ballast behavior under dynamic loading. Part 1: A 2D polygonal discrete element method approach,” Computer Methods in Applied Mechanics and Engineering, Vol. 195, No. 19-22, April, pp.2841-2859.
8. Wang, J., and Zeng, X., (2004). “Numerical simulations of vibration attenuation of high-speed train foundations with varied trackbed underlayment materials,” Journal of Vibration and Control, Vol. 10, No. 8, August, pp.1123-1136.
9. Itasca consulting group, Inc. (2002). “FLAC2D User manual (Version 4.0),” Minneapolis: Itasca Consulting Group Inc, pp. 1-4.
10. Korean National Railway (2001). “Design criteria for Railroad (Roadbed),” Korean National Railway, pp. 72-83.
11. Eum, K. Y., Koo, D. H., Yang, S. C., Yeo, I. H., Mun, H. S., Um, J. H., Sin, S. K., Kim, T. W., Kim, E., and Lee, H. S. (2005). “Development of track system innovation technology for speed-up conventional line,” Korea Railroad Research Institute. 5th Report.
12. Seo, S. (2002). “Railway engineering,” Korea: Eul & Al Press, pp.327-394.